STATISTICS, OPTIMIZATION AND INFORMATION COMPUTING
*Stat., Optim. Inf. Comput.*, Vol. **x**, Month 202x, pp 0–14.
Published online in International Academic Press (www.IAPress.org)

# On microscopic numerical simulations of an SIQR model on networks

Thabang Mapharing*, Mokaedi V. Lekgari

*Department of Mathematics and Statistical Sciences, Botswana International University of Science and Technology, Botswana*

**Abstract** This study investigates the dynamics of infectious disease spread using the Susceptible-Infected-Quarantined-Recovered (SIQR) model, integrating both classical differential equations and network theory. To capture the heterogeneous nature of real-world contact patterns, we extend mathematical formulation and analysis of the SIQR model to network-based simulations, focusing on two key network structures: the Erdős-Rényi (ER) random network and the Barabási–Albert (BA) scale-free network. Numerical simulations are performed to compare the progression of epidemics across these network types, highlighting the impact of network topology on infection spread, quarantine effectiveness, and epidemic severity. Our results demonstrate that scale-free networks, characterized by highly connected hubs, facilitate faster and more intense outbreaks compared to random networks, underscoring the importance of network structure in epidemic modeling and control strategies. This work provides a comprehensive perspective on the interplay between disease dynamics and contact network structure, offering valuable insights for the design of effective intervention policies.

**Keywords** SIQR model, Network Theory, Erdős-Rényi Network, Barabási-Albert Network, Epidemic Model, Quarantine, Basic reproduction number, COVID-19 model

**DOI:** 10.19139/soic-2310-5070-2448

## 1. Introduction

On December 31, 2019, the China Health Authority alerted the World Health Organization (WHO) about a cluster of pneumonia cases of unknown origin in Wuhan, Hubei Province [1]. These cases, which were first reported on December 8, had an initial connection to the Huanan Seafood Wholesale Market, where many affected individuals either worked or lived nearby.

On January 7, 2020, the novel coronavirus responsible for these cases was identified and temporarily named 2019-nCoV [2, 3]. Shortly thereafter, it was officially designated as severe acute respiratory syndrome coronavirus 2 (SARS-CoV-2) by the Coronavirus Study Group, and the disease caused by this virus was named coronavirus disease 2019 (COVID-19) by the WHO.

By January 30, 2020, the virus had spread significantly, with 7,736 confirmed cases and 12,167 suspected cases reported in China. In addition, 82 cases were detected in 18 other countries. On the same day, the WHO declared the SARS-CoV-2 outbreak a Public Health Emergency of International Concern (PHEIC), recognizing the potential global threat the virus poses.

Initial reports from China's National Health Commission indicated a mortality rate of 2.1% among confirmed cases, with a lower mortality rate of 0.2% among cases outside China [4, 5]. Hospitalized patients faced higher mortality rates, ranging from 11% to 15% [6]. Despite the relatively high infectiousness and moderate mortality rate of COVID-19, available data rapidly evolved as new information became available in public health reports and the scientific literature [4].

*Correspondence to: Thabang Mapharing (Email: maphathabang@gmail.com). Department of Mathematics and Statistical Sciences, Botswana International University of Science and Technology, Pvt. Bag 0016, Palapye, Botswana.

ISSN 2310-5070 (online) ISSN 2311-004X (print)

Transmission of SARS-CoV-2 occurs primarily through respiratory droplets produced when an infected person coughs, sneezes, or talks. Close contact with an infected individual is a significant risk factor, as the virus can be transmitted within households, healthcare settings, and other environments where people gather. Fomites, or contaminated surfaces, may also serve as a transmission route, as the virus has been shown to persist on surfaces for extended periods—up to 96 hours in some studies.

The possibility of asymptomatic transmission has been a topic of ongoing debate. Initial reports indicated that asymptomatic individuals might spread the virus; however, subsequent investigations revealed that some purported asymptomatic cases had unrecognized symptoms before transmission. As research continues, findings about the characteristics of the disease and its transmission dynamics are rapidly evolving. Mathematical modeling of infectious diseases has been instrumental in understanding and predicting the dynamics of epidemics like COVID-19.

The pioneering mathematical models of Kermack and McKendrick in 1927 laid the foundation for compartmental models, where populations are divided into distinct categories to simulate the spread of diseases [8]. These categories typically include susceptible individuals $S(t)$, infected individuals $I(t)$, recovered individuals $R(t)$, and, in more sophisticated models, quarantined individuals $Q(t)$, forming what is known as the Susceptible-Infected-Quarantine-Recovered (SIQR) model. These models are represented by systems of differential equations that track how individuals move between compartments over time [9].

The central objective of such models is to understand the underlying mechanisms that drive the spread of infectious diseases, predict future outbreaks and evaluate control strategies such as quarantine, vaccination and isolation. In particular, the SIQR model is designed to incorporate the dynamics of quarantining infected individuals, a crucial control measure that directly affects the progression of an epidemic by reducing the number of infectious contacts. Quarantine not only reduces the spread of the infection but also creates a separate compartment for those who are isolated, making the SIQR model a more realistic reflection of real-world epidemic management [10].

In this paper, we explore the SIQR model using both differential equations and network theory to simulate disease dynamics. While differential equations provide a macroscopic view of how populations evolve, network-based models offer a microscopic perspective, considering individual interactions that can better capture the complex and heterogeneous nature of disease spread. Networks, composed of nodes and edges, allow for a more detailed examination of the epidemic's progression through specific population structures, such as random and scale-free networks. These structures play a significant role in determining how fast and far a disease can spread, making them essential for accurate simulations.

The networks studied in this work include the Erdős-Rényi (ER) random network, where edges between nodes are randomly assigned, and the Barabási-Albert (BA) network, which follows a preferential attachment process, leading to a scale-free network structure with hubs. These models are widely used in the study of epidemic spread because they can mimic different types of social or contact networks. The ER model represents populations with uniformly random interactions, while the BA model reflects real-world systems where a few individuals (hubs) have disproportionately high number of connections. This difference in network structure can significantly influence the outcome of an epidemic simulation.

We perform numerical simulations of the SIQR model using Python, comparing the spread of the infection across both types of networks. The simulations provide insights into how the structure of a network affects disease transmission, the effectiveness of quarantine measures, and the overall dynamics of an epidemic. Finally, we present analytical and numerical solutions to the SIQR model, discussing the impact of various parameters such as the transmission rate $\beta$, quarantine rate and recovery rate. Through this approach, we aim to provide a comprehensive understanding of epidemic dynamics both from a mathematical and network-based perspective, contributing to the development of more effective strategies for controlling infectious diseases.

We give a brief review of key concepts in network theory in Section 2. A deterministic SIQR epidemic model is introduced and analysed in Section 3. In Section 4 we focus on microscopic simulations of the SIQR model on ER and BA networks. Section 5 provides a summary of our main findings, discusses their implications for epidemic modeling and intervention strategies, and outlines directions for future research.

## 2. Networks

### 2.1. Outline of Network Theory

Network theory is a branch of applied mathematics that studies the interactions and relationships between elements within a system by using a graph-theoretic representation [15]. The fundamental idea behind network theory is to model systems as networks composed of nodes, representing individual entities, and edges, representing the interactions between these entities. This approach allows researchers to understand the structure and dynamics of complex systems by examining how nodes and edges are organized and how they interact [16].

In networks, there are two fundamental components: nodes and edges. Nodes represent the individual entities within the network, such as people in a social network. Whereas edges, represent the connections, interactions, or relationships between nodes [17]. In a social network, for instance, edges could stand for either communication or friendship relationships. The degree of a node, defined as the number of connections that it has to other nodes, indicates how well-connected that node is within the network. This concept is crucial for understanding the influence of particular nodes in the network [19].

Network theory is deeply established in graph theory, which was initially developed to address problems related to connectivity and optimization. One of the earliest and most famous problems that spurred the development of graph theory was the Seven Bridges of Königsberg problem, which led to the formulation of fundamental concepts such as Eulerian paths and circuits. Network theory has emerged as a key subset, focusing on the structure and dynamics of networks in various real-world systems [20]. Networks can display various characteristics, two of them being small-world and scale-free structures. Small-world networks are distinguished by their short average path lengths and significant clustering [21]. High clustering means that nodes tend to form tightly knit groups, in which the majority of the nodes are connected. Short average path lengths indicate that any two nodes in the network can be connected by a relatively small number of steps, which enables the rapid spread of information, signals, or disturbances across the network. This property is especially important in understanding phenomena such as the spread of diseases in social networks. Scale-free systems are characterized by a power-law degree distribution, where most nodes have a few connections, but several nodes, called hubs, have a excessively large number of connections. This type of network structure was notably described by A. L. Barabási and R. Albert [15] and further investigated by A. L. Barabási [18].

Network theory provides a powerful framework for understanding the complex interactions within systems across a wide range of disciplines. By modeling systems as networks of nodes and edges, researchers can gain insights into the structure, dynamics, and vulnerabilities of these systems. The concepts of small-world and scale-free networks have been particularly influential in explaining how real-world networks function and respond to changes. As network theory continues to develop, it will likely provide even deeper insights into the complexities of interconnected systems, with applications that extend far beyond its current scope [22].

### 2.2. Network Generation

*2.2.1. Erdős-Rényi Network* The Erdős-Rényi (ER) network model is a foundational concept in the field of network theory, providing a simple yet powerful framework for understanding random graph structures. The model was independently introduced by Paul Erdős and Alfréd Rényi in 1959 [23], and by Edgar Gilbert [24] around the same time, leading to the two commonly used versions of the model. In the Erdős-Rényi model, a network is constructed by randomly connecting nodes. The model begins with a set of $n$ nodes, and each possible pair of nodes is connected by an edge with a fixed probability $p$, independently of all other pairs. This leads to a binomial distribution of the number of edges in the graph, making the model particularly useful for studying the properties of random graphs.

There are two primary variants of the Erdős-Rényi model being the $G(n,p)$ model and the $G(n,M)$ model. The $G(n,p)$ version is defined by the number of nodes $n$ and the probability $p$ that any given pair of nodes is connected by an edge. The edges are formed independently, which means the total number of edges follows a binomial distribution with parameters $\binom{n}{2}$ (the number of possible edges) and $p$. The other version, the $G(n,M)$

model, has a network constructed by randomly selecting $M$ edges from the possible $\binom{n}{2}$ edges [25]. This model is sometimes referred to as the Erdős-Rényi random graph with a fixed number of edges.

Erdős-Rényi (ER) networks are a foundational model in network theory, offering simplicity and versatility for theoretical exploration. These networks possess several key properties that make them essential for understanding the behavior of random graphs.

One of the fundamental aspects of ER networks is their degree distribution. In the $G(n, p)$ model, the degree distribution represents the number of edges connected to a node. Initially, this distribution follows a binomial pattern, but as the number of nodes $n$ increases, it approximates a Poisson distribution with a mean of $np$. This characteristic allows ER networks to effectively model the distribution of connections in random networks as they scale [26].

Another crucial property of ER networks is their connectedness. The likelihood that an ER network is fully connected—meaning there is a path between any two nodes—depends on the probability $p$. As the number of nodes $n$ grows, and $p$ is scaled according to $p = \frac{\log n}{n}$, the network undergoes a transition from being almost surely disconnected to connected. This transition is vital for understanding how connectivity emerges in random graphs and has implications for network robustness [27].

Despite their utility, ER networks typically exhibit a low clustering coefficient. The clustering coefficient measures the probability that two neighbors of a node are also neighbors of each other. In ER networks, this probability is simply $p$ and does not scale with the size of the network. As a result, ER networks often lack the high levels of clustering seen in many real-world networks, where local connections tend to be more prevalent.

Finally, Erdős-Rényi networks are characterized by their relatively short average path length between nodes, which scales logarithmically with the number of nodes, $\log n$, making ER networks "small-world" in terms of path length. Unlike Watts-Strogatz small-world networks, which combine short path lengths with high clustering coefficients to mimic local community structures, ER networks lack significant clustering and exhibit a simpler, more homogeneous random connectivity pattern. While Watts-Strogatz networks more realistically capture local clustering found in social contacts, their complex structure can introduce variability and biases in epidemic simulations, making them less suitable for studies focused on clear, comparative analysis of network effects. In contrast, ER networks provide a mathematically tractable and sufficiently simple framework that facilitates direct comparison with scale-free networks such as Barabási-Albert (BA) models, which are often used to represent heterogeneous contact patterns in epidemic modeling. This simplicity and the absence of disconnected components in ER networks make them better suited for controlled investigations of epidemic dynamics and intervention strategies, as demonstrated in recent comparative studies [23, 28].

An ER network with 50 nodes and a fixed probability $p$ of 0.1 is shown in Figure 1. It shows a comparatively even distribution of node edges. There are no obvious "hub" nodes that control the structure, however some nodes have a little more connections than others. The absence of preferred attachment throughout the development process is reflected in this connectivity's unpredictability.

*2.2.2. Barabási-Albert Network* The Barabási-Albert (BA) model is a pivotal framework in network science that describes the development of scale-free networks through a process known as preferential attachment. Introduced by Albert-László Barabási and Réka Albert in 1999 [15], this model has significantly advanced our understanding of the growth and evolution of complex networks, such as those found in the World Wide Web, social networks, and biological systems.

The BA model generates random networks that exhibit a scale-free structure, meaning that their degree distribution follows a power law. In simpler terms, most nodes in these networks have relatively few connections, while a small number of nodes, known as hubs, have a large number of connections. This pattern mirrors many real-world networks, making the BA model particularly useful for studying their dynamics and structure[18].

The Barabási–Albert model operates on two core principles: growth and preferential attachment. The network begins with a small number of nodes, and new nodes are continuously added, one at a time. When a new node joins the network, it is more likely to connect to nodes that are already well-connected, rather than connecting randomly to any existing node. The probability that a new node will link to an existing node is proportional to the number of connections that node already has [29]. This mechanism, known as preferential attachment, captures

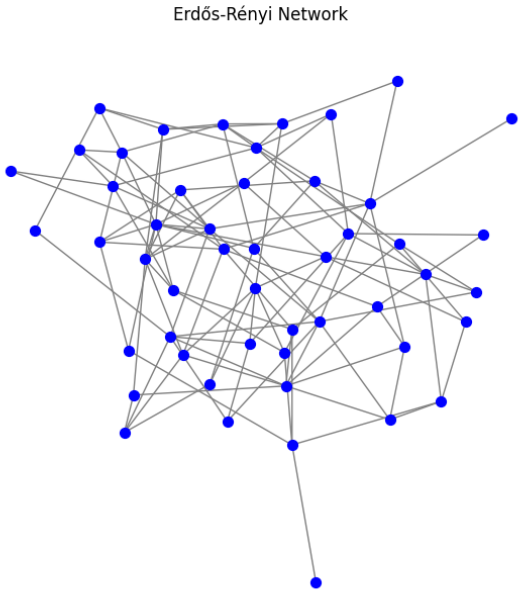


Figure 1. The ER network with N=50 , p=0.1

the "rich-get-richer" phenomenon, where well-connected nodes are more likely to attract even more connections, leading to the emergence of hubs in the network.

Barabási–Albert networks display several distinctive properties that set them apart from other types of networks. The most notable feature is their power-law degree distribution, where the likelihood of a node having a certain number of connections decreases as a power of that number. This results in a network where most nodes have few connections, while a few nodes serve as highly connected hubs. These networks are robust against random failures, meaning that removing a random node is unlikely to disrupt the network significantly. However, they are vulnerable to targeted attacks on the hubs, which can fragment the network.

Despite the presence of hubs, BA networks exhibit the small-world effect, where the average path length between nodes is relatively short, scaling logarithmically with the size of the network. Additionally, the diameter of a BA network, which is the longest shortest path between any two nodes, is also relatively small, reflecting the efficiency of communication within the network [30]. Overall, the Barabási-Albert model provides a powerful framework for understanding the complex, self-organizing structures that characterize many real-world networks.
A BA network with 50 nodes and an average of 8 connections is shown in Figure 2. It has several "hub" nodes, some of which are substantially more connected than others. The structure is dominated by these densely connected nodes, which are also essential to the overall connectivity of the network.

## 3. Theoretical Framework

### *3.1. Deterministic SIQR Model*

The foundational work on mathematical modeling of infectious diseases was laid out by Kermack and McKendrick in 1927 [8]. Their simple epidemic model has since become a cornerstone for subsequent research in the field. In studying these mathematical models, the population is typically divided into several categories: susceptible individuals $S(t)$, infected individuals $I(t)$, and recovered individuals $R(t)$.

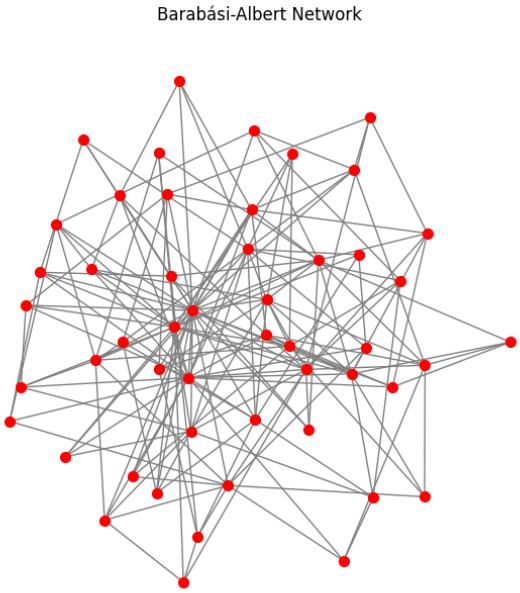


Figure 2. The BA network with N=50, k=8

$$\begin{cases} \frac{dS(t)}{dt} = -\beta S(t)I(t) \\ \frac{dI(t)}{dt} = \beta S(t)I(t) - rI(t) \\ \frac{dR(t)}{dt} = rI(t) \end{cases} \tag{1}$$

With the addition of a Quarantined compartment to the SIR model we have a Susceptible – Infected – Quarantine – Recovered (SIQR) epidemic model. The SIQR disease transmission model is derived assuming several strong assumptions. Individuals who are Susceptible in this model are those who are at risk of becoming infected. Quarantine is defined as isolating an infected person who exhibits signs of the disease.Quarantine is defined as an infected person who exhibits signs of the disease and is isolated. Quarantined individuals who recover from the disease are considered as Recovered. One interesting example of an SIQR model is one governed by the following set of differential equations:

$$\begin{cases} \frac{dS(t)}{dt} = A - \mu S(t) - \frac{\beta S(t)I(t)}{N(t)} \\ \frac{dI(t)}{dt} = \frac{\beta S(t)I(t)}{N(t)} - (d + r + \mu)I(t) \\ \frac{dQ(t)}{dt} = rI(t) - (\epsilon + \mu)Q(t) \\ \frac{dR(t)}{dt} = dI(t) + \epsilon Q(t) - \mu R(t) \end{cases} \tag{2}$$

In these equations, $Q(t)$ represents the quarantined individuals at time $t$, while $S(t)$, $I(t)$, and $R(t)$ denote the susceptible, infected, and recovered populations, respectively. The transitions between these compartments and the associated parameters are illustrated in Figure 3, which provides a schematic overview of the SIQR model dynamics.

In the deterministic SIQR model, we assume homogeneous mixing, meaning each individual is equally likely to interact with any other individual in the population. While this assumption simplifies the mathematical analysis, it does not capture the heterogeneous and structured nature of real-world contact patterns. To address this limitation, we subsequently explore network-based SIQR models that incorporate more realistic interaction structures.

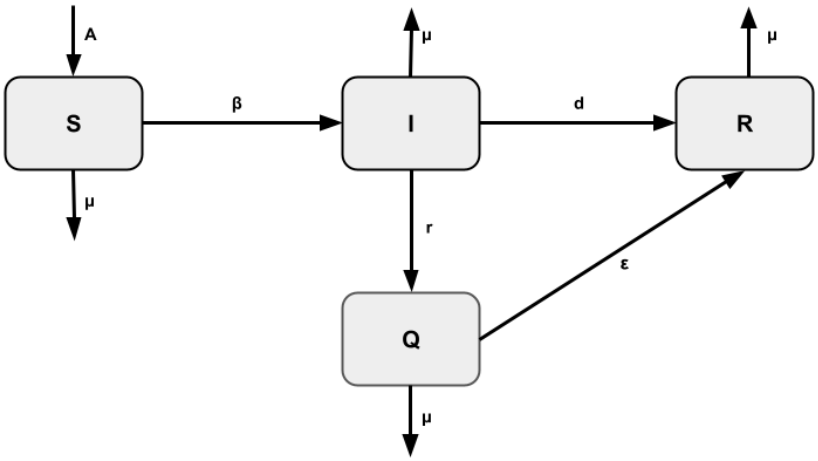


Figure 3. Diagram showing the transitions from Susceptible to Recovered.

### *3.2. Parameter Estimation*

The model parameters used in this study were chosen based on values commonly reported in the epidemiological literature and, where necessary, adjusted to reflect the characteristics of the SIQR framework. These values provide a basis for our simulations and allow for meaningful comparison of epidemic dynamics across different network structures. The table below summarizes the parameter values used throughout our analysis.

| **Parameter** | **Meaning** | **Typical Range (COVID-19)** | **Reference/Notes** |
|---|---|---|---|
| $\beta$ | Transmission rate (probability of disease transmission per contact per day) | 0.3 – 1.5 per day | [33]; [34]; context-dependent, affected by interventions |
| $r$ | Quarantine rate (rate of identifying and isolating infected individuals) | 0.05 – 0.3 per day | [35]; depends on testing/tracing efficiency |
| $d$ | Recovery rate for non-quarantined infected individuals | 0.07 – 0.2 per day | [34]; corresponds to infectious period of 5–14 days |
| $\epsilon$ | Recovery rate for quarantined individuals | 0.07 – 0.2 per day | Assumed similar to $d$; may vary with healthcare quality |
| $\mu$ | Natural death rate (unrelated to the disease) | $2.7 \times 10^{-5}$ – $3.8 \times 10^{-5}$ per day | World Bank Data; global annual crude death rate |
| $A$ | Recruitment/immigration rate | $\approx \mu \times N$ (to keep population stable) | Model assumption; $N$ is total population |

Table 1. Summary of SIQR model parameters, their meanings, typical empirical ranges, and references.

### *3.3. Reproductive Number*

The four compartments make up the total population of N(t):

$$N(t) = S(t) + I(t) + Q(t) + R(t).$$

In mathematical problems involving infectious diseases, the basic reproduction number, also called the basic reproduction rate or the basic reproduction ratio, is a useful threshold parameter. This metric is useful because it helps determine whether or not an infectious disease will spread through a population. In this section, we will use the next-generation matrix method to compute the model's basic reproduction number, $R_0$ [31, 32]. For that, we rewrite the model as $\frac{dx}{dt} = \mathbb{F}(x) - \mathbb{A}(x)$ where $x$ = (S I Q R).

$$\mathbb{F}(x) = \begin{bmatrix} \frac{\beta SI}{N} \\ 0 \\ 0 \\ 0 \end{bmatrix} \text{ and } \mathbb{A}(x) = \begin{bmatrix} (\mu + d + r)I(t) \\ -rI(t) + (\mu + \varepsilon)Q(t) \\ -dI(t) - \varepsilon Q(t) + \mu R(t) \\ -A + \mu S(t) + \frac{\beta S(t)I(t)}{N(t)} \end{bmatrix}.$$

We have the Jacobian matrices for $\mathbb{F}$(x) and $\mathbb{A}$(x) at the disease-free equilibrium $E_0 = (\frac{A}{\mu}, 0, 0, 0)$ as **F** and **V** respectively:

$$\mathbf{F}= \begin{bmatrix} \frac{\beta}{N} & 0 & 0 & 0 \\ 0 & 0 & 0 & 0 \\ 0 & 0 & 0 & 0 \\ 0 & 0 & 0 & 0 \end{bmatrix}., \mathbf{V}= \begin{bmatrix} (\mu + d + r) & 0 & 0 & 0 \\ -r & (\mu + \varepsilon) & 0 & 0 \\ d & -\varepsilon & \mu & 0 \\ \frac{\beta}{N} & 0 & 0 & \mu \end{bmatrix}.$$

$FV^{-1}$ is the next generation matrix for the model. It then follows that the spectral radius of matrix $FV^{-1}$ is $\rho(FV^{-1}) = \frac{\beta}{\mu+d+r}$. Thus, the basic reproduction number of the model is given by

$$R_0 = \frac{\beta}{\mu + d + r}. \tag{3}$$

The value $R_0$ represents the average number of secondary infections when an infected person enters a fully susceptible population. When $R_0 \leq 1$, the number of infected individuals decreases, and the model has only a disease-free equilibrium, which is globally asymptotically stable [36]. This indicates that the disease will eventually die out, and the entire population will recover. On the other hand, when $R_0 > 1$, the number of infected individuals increases, and the disease-free equilibrium becomes unstable, leading the model to have only the endemic equilibrium, which is globally asymptotically stable.

### *3.4. Properties of the Model*

Summing up all the equations of the model (2), we find the following differential equations $S(t)$, $I(t)$, $Q(t)$, and $R(t)$, then get:

$$\frac{dN(t)}{dt} = \frac{dS(t)}{dt} + \frac{dI(t)}{dt} + \frac{dQ(t)}{dt} + \frac{dR(t)}{dt}.$$

Then substitute each equation:

$$\frac{dN(t)}{dt} = \left(A - \mu S(t) - \frac{\beta S(t)I(t)}{N}\right) + \left(\frac{\beta S(t)I(t)}{N} - (\mu + d + r)I(t)\right) + (rI(t) - (\mu + \epsilon)Q(t))$$

$$+ (dI(t) + \epsilon Q(t) - \mu R(t)).$$

Simplifying:

$$\frac{dN(t)}{dt} = A - \mu S(t) - (\mu + d + r)I(t) + rI(t) - (\mu + \epsilon)Q(t) + dI(t) + \epsilon Q(t) - \mu R(t),$$

$$\frac{dN(t)}{dt} = A - \mu S(t) - \mu I(t) - \mu Q(t) - \mu R(t),$$

$$\frac{dN(t)}{dt} = A - \mu(S(t) + I(t) + Q(t) + R(t)).$$

Since $N(t) = S(t) + I(t) + Q(t) + R(t)$,

$$\frac{dN(t)}{dt} = A - \mu N(t).$$

This equation describes the total population dynamics, accounting for births (at rate $A$) and natural deaths (at rate $\mu$). This denotes that population size $N \to \frac{A}{\mu}$ as t $\to \infty$.

By comparison theorem, we obtain that the solutions of model (2) exist in the region defined by

$$\Gamma = \left\{(S, I, Q, R) \in \mathbb{R}^4_+ : S + I + Q + R \leq \frac{A}{\mu}, S \geq 0, I \geq 0, Q \geq 0, R \geq 0\right\}.$$

### *3.5. Numerical Simulations*

In this section, we give some numerical simulations to illustrate the theoretical model. A Python program is used to solve the system of the SIQR model. For the initial conditions, we set total population, S(0)=990, initial infected, I(0) = 10, Q(0) = 0 initial quarantined and R(0) = 0 initial recovered. For the parameters, we set birth rate A = 10, natural death rate $\mu$ = 0.01, recovery rate of infected individuals d = 0.05, quarantine rate r = 0.1, recovery rate of quarantined individuals $\epsilon$ = 0.05 and initial total population N(0) = 1000. In the simulations, time is treated as a stochastic variable, with events occurring at random intervals determined by the relevant transition rates. The values for the parameter of $\beta$ were varied for 0.3, 0.5, 0.7, and 0.9.

## 4. Microscopic Simulations of the SIQR Model on Networks

### *4.1. Calculation of the Basic Reproduction Number* $R_0$

Before presenting the simulation results, we calculate the basic reproduction number $R_0$ for both the Erdős-Rényi (ER) and Barabási-Albert (BA) networks, as this metric provides a threshold indicator for epidemic outbreaks and is essential for interpreting the observed dynamics.

The basic reproduction number for the SIQR model on a network is given by [37]:

$$R_0 = \frac{\beta}{r + d + \mu}\langle k\rangle \tag{4}$$

where $\langle k\rangle$ is the average degree of the network.

For the ER network, the average degree is $\langle k\rangle = np = 1000 \times 0.01 = 10$. Substituting the parameter values ($\beta = 0.4$, $r = 0.1$, $d = 0.05$, $\mu = 0.01$), we obtain:

$$R_0^{ER} = \frac{0.4}{0.1 + 0.05 + 0.01} \times 10 = \frac{0.4}{0.16} \times 10 = 2.5 \times 10 = 25.$$

For the BA network, the average degree is $\langle k\rangle = 2m = 14$ (with $m = 7$).
Thus,

$$R_0^{BA} = \frac{0.4}{0.1 + 0.05 + 0.01} \times 14 = \frac{0.4}{0.16} \times 14 = 2.5 \times 14 = 35.$$

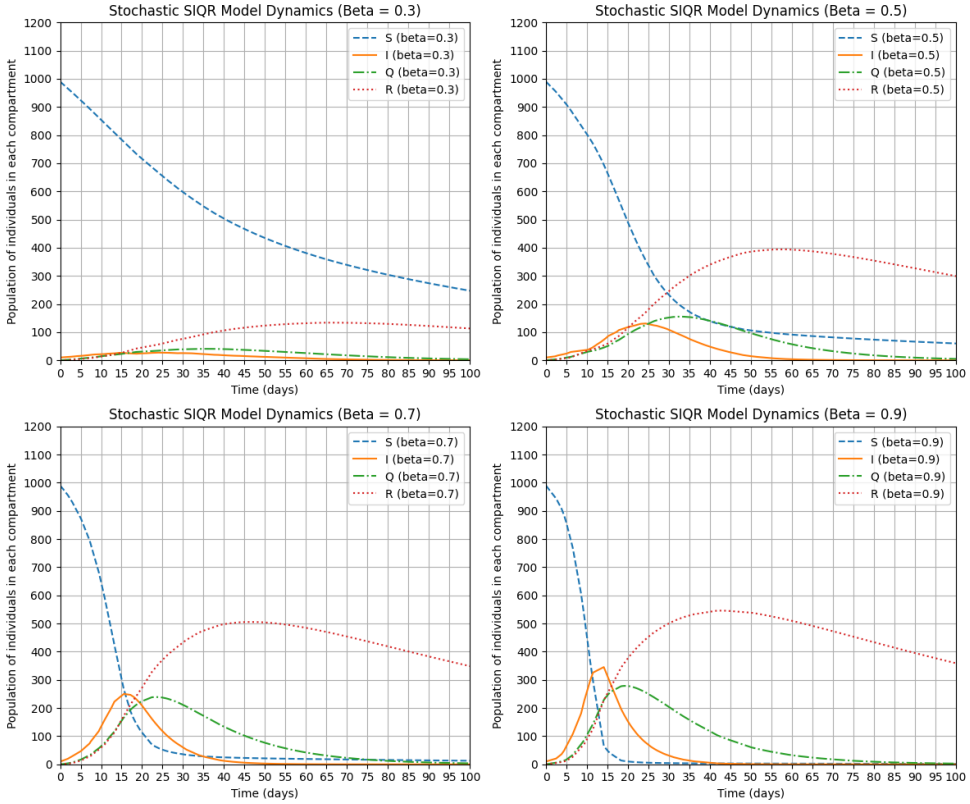


Figure 4. Time evolution of the SIQR epidemic model simulated using stochastic time steps, reflecting random infection events and transitions.

These results show that the basic reproduction number is higher in the BA (scale-free) network due to its higher average degree, reflecting the increased risk of epidemic outbreaks in heterogeneous networks. The high $R_0$ values do not necessarily reflect realistic COVID-19 or other disease scenarios, but rather illustrate the theoretical epidemic potential under the selected parameters and network structures. The results underscore the importance of both parameter selection and network structure in determining epidemic risk. In particular, the combination of high transmission rates and dense or heterogeneous connectivity in these network models amplifies $R_0$, highlighting how changes in model assumptions or contact patterns can dramatically affect outbreak potential.

### *4.2. Erdős-Rényi Network Simulations*

In this section, we perform a microscopic simulation of the SIQR model on an Erdős-Rényi (ER) network. The parameters of the simulations correspond to those used in the differential equations describing the macroscopic behavior of the system. The simulations follow Algorithm 1. They involve generating a static network, initializing infections, and simulating stochastic infection, quarantine, and recovery dynamics over time.

[1] **Generate Network**: Create a static Erdős-Rényi network with a fixed number of nodes and connection probability. **System Initialization**: Infect 10 random nodes at $t = 0$.

simulation is running **Infection Dynamics**: 4.1 With probability $p$, a susceptible individual (S) gets infected (I) if one of its neighbors is infected. 4.2 Quarantine a random proportion of infected individuals (I).

**Recovery Dynamics**: 5.1 Infected individuals recover after $1/d$ days, following a Poisson distribution. 5.2 Quarantined individuals recover after $1/\epsilon$ days, following a Poisson distribution. **Iteration**: At each time step $t$, steps 4 and 5 are executed based on stochastically determined time intervals, simulating infection, quarantine, and recovery within the network.

### *4.3. Barabási-Albert Network Simulations*

In this section, we perform a microscopic simulations of the SIQR model on an Barabási-Albert (BA) network. The parameters of the simulations correspond to those used in the differential equations describing the macroscopic behavior of the system. The simulation The simulations, as per Algorithm 2, we extend the mathematical SIQR model simulations to a Barabási-Albert network. It follows a similar process, incorporating preferential attachment to capture realistic network dynamics, emphasizing stochastic transitions between compartments.

[1] **Network Generation**: Generate a Barabási-Albert network with fixed parameters, including number of nodes and edges $M$ for each new node.

**Initial Infections** ($t = 0$): Infect 10 random nodes in the network.

simulation is running **Infection Dynamics**: 4.1 A susceptible individual (S) gets infected (I) with probability $p$ if one of its $k$ neighbors is infected. 4.2 Quarantine a random proportion of infected individuals (I).

**Recovery Dynamics**: 5.1 Infected individuals recover after $1/d$ days, following a Poisson distribution. 5.2 Quarantined individuals recover after $1/\epsilon$ days, also following a Poisson distribution.

**Iteration**: At each time step $t$, steps 4 and 5 are executed, simulating infection, quarantine, and recovery dynamics.

**Simulation Sampling**: Perform the simulation over 20 independent samples to ensure reliable results.

Algorithm 4.3 extends the SIQR simulation to a

### *4.4. Global Sensitivity Analysis*

Understanding which parameters most strongly influence the epidemic dynamics is essential for both model interpretation and effective intervention planning. To this end, we performed a global sensitivity analysis of the microscopic SIQR model using Sobol indices, a variance-based technique that quantifies the contribution of each parameter and their interactions to the variability observed in model outputs.

The Sobol method provides a systematic framework for assessing the relative importance of each parameter across their entire plausible ranges, rather than relying on local, one-at-a-time perturbations. In our analysis, we considered the following model parameters: the transmission rate ($\beta$), the quarantine rate ($r$), the recovery rates ($d$ for infected and $\epsilon$ for quarantined individuals), and the natural death rate ($\mu$). Each parameter was varied within a biologically reasonable range, while the model was simulated repeatedly on both Erdős–Rényi (ER) and Barabśi–Albert (BA) networks.

For each simulation, key epidemic outcomes were recorded, including the peak number of infected individuals, the total number of recovered individuals at the end of the simulation, and the time to epidemic peak. The Sobol indices were then computed to determine the proportion of output variance attributable to each parameter and to their higher-order interactions.

| **Parameter** | **ER** $S_1$ | **BA** $S_1$ | **ER** $S_T$ | **BA** $S_T$ |
|---|---|---|---|---|
| $\beta$ | 0.336 | 0.182 | 0.523 | 0.626 |
| $r$ | 0.328 | 0.413 | 0.642 | 0.848 |
| $d$ | 0.012 | 0.055 | 0.425 | 0.390 |

Table 2. First-order ($S_1$) and total effect ($S_T$) Sobol indices for each parameter on ER and BA networks.

The Sobol sensitivity analysis indicates that both the transmission rate ($\beta$) and the quarantine rate ($r$) are highly influential in determining epidemic outcomes across both network types. For the ER network, the first-order indices show that $\beta$ (0.336) and $r$ (0.328) contribute almost equally to the variance in the final epidemic size, while for the BA network, $r$ (0.413) is more influential than $\beta$ (0.182). The total effect indices ($S_T$) further highlight the importance of $r$, especially in the BA network, where it accounts for approximately 85% of the variance, indicating strong interaction effects.

The recovery rate ($d$) has a relatively minor first-order effect, but its total effect is substantial (0.425 for ER and 0.390 for BA), suggesting that $d$ primarily influences outcomes through interactions with other parameters.

Overall, these results reveal that both transmission and quarantine rates are critical drivers of epidemic dynamics, with quarantine playing an even more dominant role in scale-free (BA) networks. This underlines the importance of rapid quarantine measures and early transmission suppression to effectively control epidemic spread, especially in heterogeneous networks where super-spreader nodes may exist.

### *4.5. Results of SIQR Model on Erdős-Rényi Network*

We performed a simulation of the microscopic SIQR model on the Erdős-Rényi (ER) network over a time of 100 days. In Figure 5, the temporal variations of the number of individuals in four compartments—Susceptible (S), Infected (I), Quarantined (Q), and Recovered (R)—are plotted. The average number of connections per node is $\langle k \rangle$ = 10, and the edge probability $p$ is set to 0.01. The parameters $\beta$, $r$, $d$, $\epsilon$ and $\mu$ were chosen to be consistent with the numerical solution of the macroscopic SIQR model.

The Erdős–Rényi (ER) network consists of 1,000 nodes, with 10 individuals randomly selected as initially infected. Due to the homogeneous connectivity of the ER network, where each node has a roughly equal probability of interacting with any other, the spread of infection is gradual and relatively uniform across the population. The peak number of infected individuals reaches approximately 508, occurring at about 6.8 days, which is later than in the BA network. The final epidemic size, represented by the total number of recovered individuals, is around 824. This results in a smooth, moderate epidemic curve, with the quarantined and recovered populations rising steadily in response to the slower and more evenly distributed transmission dynamics characteristic of random networks.

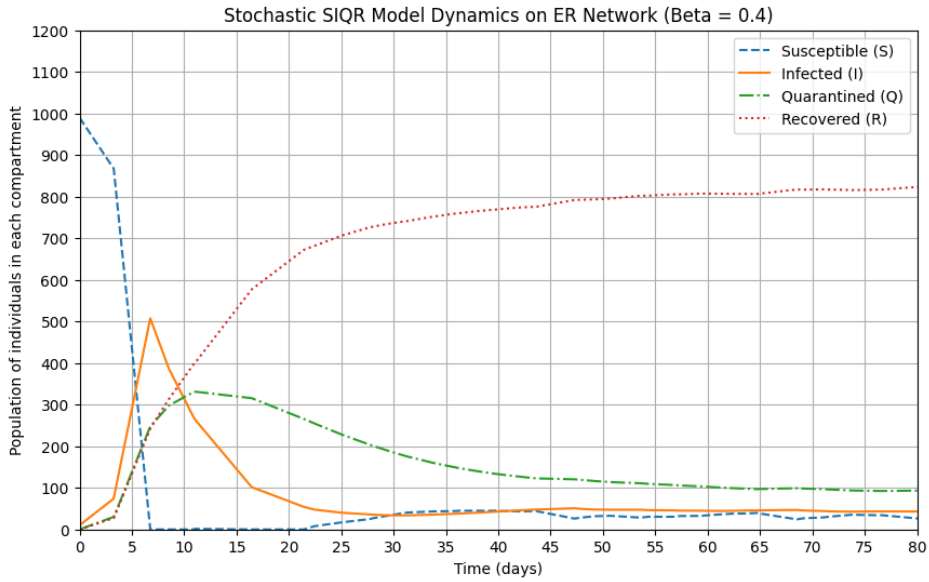


Figure 5. Time evolution of the number of susceptible (S), infected (I), quarantined (Q), and recovered (R) individuals in a Erdős Rényi (ER) network

### *4.6. Results of SIQR Model on Barabási-Albert Network*

We also performed a simulation of the microscopic SIQR model on the Barabási-Albert (BA) network over a time of 100 days. In Figure 6, the temporal variations of the number of individuals in the compartments—Susceptible (S), Infected (I), Quarantined (Q), and Recovered (R)—are plotted. The number of edges created with each new node $m$ is set to 7. The same parameters $\beta$, $r$, $d$, $\epsilon$ and $\mu$ were applied as in the ER network simulation.

The Barabási-Albert (BA) network, consisting of 1,000 nodes with 10 initially infected individuals, is characterized by the presence of a few highly connected hubs. This structural feature leads to a rapid and uneven spread of infection, as these hubs act as super-spreaders within the network. The simulation results reflect this dynamic: the peak number of infected individuals reaches approximately 723, with the epidemic peaking very early at around 4.9 days. The final epidemic size, measured by the total number of recovered individuals, is about 843. Compared to the ER network, the BA network produces a much sharper and earlier epidemic peak, and the quarantined and recovered compartments exhibit more abrupt changes. Overall, the presence of hubs in the BA network significantly accelerates transmission, resulting in a steeper and more intense epidemic curve.

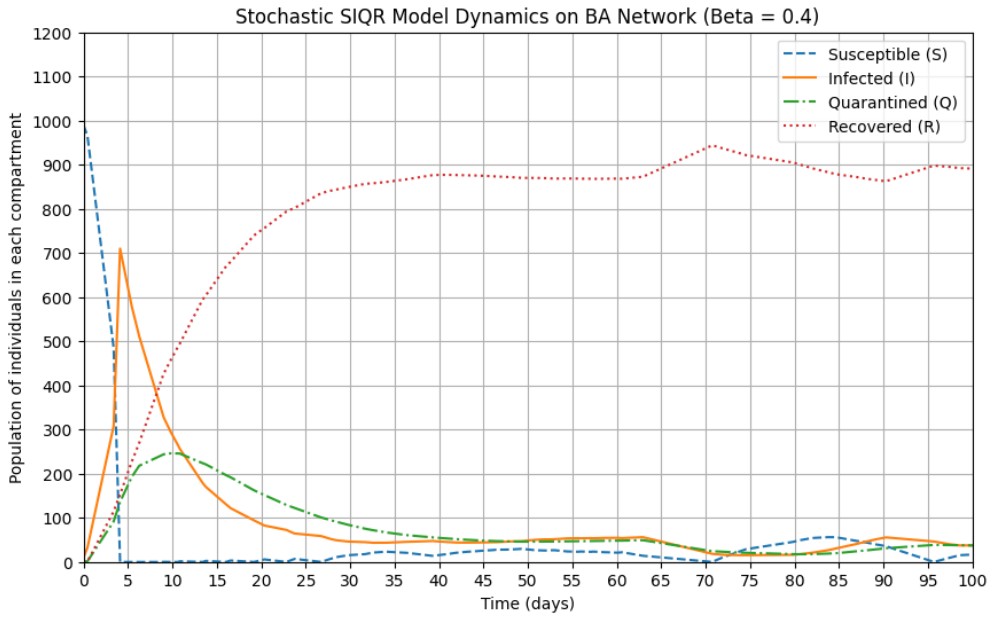


Figure 6. Time evolution of the number of susceptible (S), infected (I), quarantined (Q), and recovered (R) individuals in a Barabási–Albert (BA) network

## 5. Conclusion

We performed simulations on both networks with varying parameters that govern disease transmission, quarantine, and recovery rates. These simulations allowed us to visualize the temporal evolution of the population in each compartment (S, I, Q, R), helping us to explore the role that network connectivity plays in the epidemic's progression. By using 40 samples for each network type, we managed to capture the variation in outcomes across different network realizations.

We investigate the SIQR (Susceptible-Infected-Quarantined-Recovered) model for the spread of infectious diseases, focusing on the effects of quarantine in controlling the transmission of epidemics. We aimed to study how the structure of underlying social networks impacts the spread of diseases by applying the SIQR model to two types of network structures: Erdős-Rényi (ER) random networks and Barabási-Albert (BA) scale-free networks.

Our work focuses on the role of host quarantine/isolation within a broad epidemiological framework. Quarantine has been used to reduce the transmission of diseases for many centuries. In this paper, we have studied the dynamics of an SIQR epidemiological model. The mathematical analysis shows that the model has a disease-free equilibrium which is globally stable whenever control is effective, that is, when $R_0 \leq 1$ and otherwise it is unstable. Furthermore, it is shown that this model has a unique endemic equilibrium with the disease being uniformly persistent as long as $R_0 > 1$.

By applying the model to both the Erdős-Rényi (ER) random network and the Barabási-Albert (BA) scale-free network, distinct patterns were observed. The BA network, because of its highly connected hubs, accelerated the spread of infection, causing rapid and concentrated outbreaks. Thus, it is important for authorities to identify highly connected hubs early and educate, monitor, isolate, or give them preventive treatment as an intervention strategy. In comparison, the ER network portrayed a more evenly distributed spread, mimicking events where all individuals have approximately equal chances of interaction. While the homogeneous mixing assumption in classical compartmental models (such as the deterministic SIQR ODE framework) makes analytical work easier, it fails to capture the heterogeneity found in real-world populations, where contact patterns are influenced by factors such as age, spatial proximity, and social structure. Furthermore, the current model does not explicitly account for asymptomatic transmission, which has been shown to play an important role in the spread of diseases such as COVID-19 and can result in undetected community spread. To address these shortcomings, future research might include age-structured or geographically explicit models, as well as extra compartments for asymptomatic individuals, to give a more nuanced and realistic picture of epidemic dynamics and to guide focused intervention methods.

The results of our simulations suggest that in scale-free (BA) networks, a small number of highly connected individuals (hubs) play a disproportionate role in driving epidemic spread. This observation has clear consequences for public health policy; for example, targeting and isolating highly connected individuals within certain communities might drastically lower transmission rates. This reinforces the importance of quarantine methods adapted to network architecture, which might assist to manage epidemics more effectively. Furthermore, the model may be used to estimate the impact of super-spreader events or the advantages of improved contact tracing in heterogeneous networks. Our findings are qualitatively comparable with those of previous network-based SEIQR models, which demonstrate that network heterogeneity, particularly the presence of highly connected nodes, is a crucial factor influencing epidemic severity and disease transmission rate.

Some limitations in this model are the assumption of constant infection rates and limited changes in network structure over time, both of which could vary in real-world epidemics. This model can be improved by incorporating variable transmission rates and an evolving network structure. By blending concepts from network theory with epidemic modeling, a more detailed perspective on the role of quarantine within complex social networks can be understood. The insights acquired here could guide the development of more effective interventions, offering a clearer view of how network properties influence epidemic control strategies.

The SIQR network modeling approach proposed in this study is easily extensible to a variety of viral illnesses other than COVID-19. The model may be calibrated to represent the epidemiological features of illnesses such as seasonal influenza, measles, and newly emerging pathogens by adjusting critical factors such as the transmission rate, recovery rate, and quarantine efficacy. Furthermore, the model structure may be expanded to incorporate disease-specific compartments, such as asymptomatic carriers or vaccinated individuals. This adaptability enables the SIQR framework to influence public health initiatives for a wide range of epidemic situations, giving significant insights into both current and new infectious threats.

## Acknowledgement

Supported by Botswana International University of Science and Technology Research Grant BIUST/RI/2/2020.

REFERENCES

1. World Health Organization, *Pneumonia of unknown cause – China [Internet]*, Available from: https://www.who.int/csr/don/05-january-2020-pneumonia-of-unkown-cause-china/en/, 2020.
2. Centers for Disease Control and Prevention, *Novel coronavirus 2019, Wuhan, China [Internet]*, Available from: https://www.cdc.gov/coronavirus/novel-coronavirus-2019.html, 2020.
3. World Health Organization, *WHO Statement Regarding Cluster of Pneumonia Cases in Wuhan, China [Internet].*, Available from: https://www.who.int/china/news/detail/09-01-2020-who-statement-regarding-cluster-of-pneumonia-cases-in-wuhan-china, 2020.
4. H. Harapan, N. Itoh, A. Yufika, W. Winardi, S. Keam, H. Te, D. Megawati, Z. Hayati, A. L. Wagner, M. Mudatsir, *Coronavirus disease 2019 (COVID-19): A literature review*, Journal of Infection and Public Health, Volume 13, Issue 5, Pages 667-673, 2020.

5. T. F. Chan, and S. Esedoglu, *NHS press conference, February 4, 2020. Beijing, China*, National Health Commission (NHC) of the People's Republic of China, 2020.
6. N. Chen, M. Zhou, X. Dong, J. Qu, F. Gong, Han Y., Y. Qiu, J. Wang, Y. Liu, Y. Wei, J. Xia, T. Yu, X. Zhang, L. Zhang, *Epidemiological and clinical characteristics of 99 cases of 2019 novel coronavirus pneumonia in Wuhan, China: a descriptive study.*, The Lancet, Volume 395, Issue 10223, 507 - 513, 2020.
7. J. Xu, T. Zhang, *Dynamic Analysis for a SIQR Epidemic Model with Specific Nonlinear Incidence Rate*, Journal of Applied Mathematics and Physics, 7, 1840-1860, 2019.
8. W. O. Kermack, A. G. McKendrick, *Contribution to the mathematical theory of epidemics I*, Proceedings of the royal society of london. Series A, Containing papers of a mathematical and physical character, 115(772), 700-721., 1927.
9. H. Hethcote, M. ZhieN, L. Shengbing, *Effects of quarantine in six endemic models for infectious diseases*, Mathematical Biosciences, Volume 180, Issues 1–2, Pages 141-160, 2002.
10. Kazempour Dizaji, M., Emamhadi, M. A., Roozbahani, R., Varahram, M., Abedini, A., Zare, A., Marjani, M., *Investigating the effect of health measures and social restrictions on the COVID-19 epidemic based on the SIQR mathematical model*, Health Science Monitor, 2(4), 225-232, 2023.
11. A. Barabási, *Network Science*, Vol. 3. Cambridge, UK:: Cambridge University Press, 2016.
12. Anderson R.M., May R.M., *Infectious Diseases of Humans: Dynamics and Control*, Oxford University Press, 1991.
13. Hethcote H. W., Lewis M. A., van den Driessche P., *An epidemiological model with a delay and a nonlinear incidence rate*, Journal of mathematical biology, 27(1), 49-64., 1989.
14. Bailey N.T.J., *The Mathematical Theory of Infectious Disease*, Griffin, London, 1975.
15. Barabási, A.-L., Albert, R., *Emergence of scaling in random networks*, Science, 286(5439), 509-512, 1999.
16. Newman M., *Networks: An Introduction*, Oxford University Press, 2010.
17. Boccaletti, S., Latora, V., Moreno, Y., Chavez, M., Hwang, D. U., *Complex networks: Structure and dynamics*, Physics reports, 424(4-5), 175-308, 2006.
18. Barabási, A.-L., *Scale-free networks: A decade and beyond*, Science, 325(5939), 412-413, 2009.
19. Dunne, J. A., Williams, R. J., Martinez, N. D., *Network structure and biodiversity loss in food webs: robustness increases with connectance*, Ecology Letters, 2002.
20. Williams, R. J., Martinez, N. D., *Simple rules yield complex food webs*, Nature, 404(6774), 180-183, 2002.
21. Watts, D. J., Strogatz, S. H., *Collective dynamics of 'small-world' networks*, Nature, 393(6684), 440-442, 1998.
22. Yackinous, W., *Network Theory: The Structure of Complex Network*, Academic Press, 125-150, 2015.
23. Erdős, P., Rényi, A., Publicationes Mathematicae (Debrecen), 6, 290-297, 1959.
24. Gilbert E. N., *Random graphs*, The Annals of Mathematical Statistics, 30(4), 1141-1144, 1959.
25. Bollobás, B., *Random Graphs (2nd ed.)*, Cambridge University Press, 2001.
26. Erdős, P., Rényi, A., *On the Evolution of Random Graphs*, Publications of the Mathematical Institute of the Hungarian Academy of Sciences, 5, 17-61, 1960.
27. Janson, S., Łuczak, T., Rucinski, A., *Wiley-Interscience Series in Discrete Mathematics and Optimization*, In Random Graphs, 2000.
28. Kuryliak, Y., Emmerich, M., Dosyn, D., *On the Effect of Complex Network Topology in Managing Epidemic Outbreaks*, CEUR Workshop Proceedings, 2021.
29. Newman, M. E. J., *Networks: An Introduction*, Oxford University Press, 2018.
30. Albert, R., Barabási, A. L., *Statistical mechanics of complex networks*, Reviews of Modern Physics, 74(1), 47–97, 2002.
31. Diekmann O., Heesterbeek J.A.P., Roberts M.G., *The construction of next-generation matrices for compartmental epidemic models*, J R Soc Interface. ;7(47):873–885, 2009.
32. Van den Driessche P., Watmough J., *Reproduction Numbers and Sub-threshold Endemic Equilibria for Compartmental Models of Disease Transmission*, Mathematical Biosciences, 180, 29-48, 2002.
33. Zhu, N., Zhang, D., Wang, W., Li, X., Yang, B., Song, J., ... & Tan, W., *A novel coronavirus from patients with pneumonia in China*, New England journal of medicine, 382(8), 727-733, 2020.
34. Verity, R., Okell, L. C., Dorigatti, I., Winskill, P., Whittaker, C., Imai, N., ... & Ferguson, N. M., *Estimates of the severity of coronavirus disease 2019: a model-based analysis*, The Lancet infectious diseases, 20(6), 669-677, 2020.
35. Hellewell, J., Abbott, S., Gimma, A., Bosse, N. I., Jarvis, C. I., Russell, T. W., ... & Eggo, R. M., *Feasibility of controlling COVID-19 outbreaks by isolation of cases and contacts*, The Lancet Global Health, 8(4) 488-496, 2020.
36. Cao Z., Feng W., Wen X., Zu L., Cheng M., *Dynamics of a stochastic SIQR epidemic model with standard incidence*, Physica A: Statistical Mechanics and its Applications, Volume 527, 2019.
37. Pastor-Satorras, R., Castellano, C., Van Mieghem, P., & Vespignani, A., *Reviews of modern physics, 87(3), 925-979*, Epidemic processes in complex networks, 2015.
38. Groendyke, C. & Combs, A., *Modifying the network-based stochastic SEIR model to account for quarantine: an application to COVID-19*, Epidemiologic Methods, 10(s1), 2021.